We are IntechOpen,
the world's leading publisher of
Open Access books
Built by scientists, for scientists

4,800
Open access books available

122,000
International authors and editors

135M
Downloads

Our authors are among the

154
Countries delivered to

TOP 1%
most cited scientists

12.2%
Contributors from top 500 universities

BOOK CITATION INDEX
CLARIVATE ANALYTICS
INDEXED

WEB OF SCIENCE™

Selection of our books indexed in the Book Citation Index
in Web of Science™ Core Collection (BKCI)

Interested in publishing with us?
Contact book.department@intechopen.com

Bismuth-Based Nano- and Microparticles in X-Ray Contrast, Radiation Therapy, and Radiation Shielding Applications

Hayden Winter, Anna L. Brown and
Andrea M. Goforth

Additional information is available at the end of the chapter

Abstract

Bismuth has gained attention in preclinical research because of its ability to attenuate X-rays and high biocompatibility, which make it an excellent element for use in a biomedical agent or in radiation shielding. Developments in the synthesis of elemental bismuth nano- and microparticles, their X-radiation interactions, and their biological interactions will be reviewed in this chapter. The chapter will pay special focus to emerging medical applications of elemental bismuth nano- and microparticles, including the possibility of targeted molecular X-ray imaging, photo-thermal and X-radiation dose enhancing therapies for cancer treatment, and the construction of flexible radiation shielding materials and X-ray opaque devices.

Keywords: bismuth nanomaterial, contrast agent, therapeutic, X-ray imaging, X-ray shielding

1. Introduction to X-ray attenuating materials for medical applications

Ionizing radiation is used in many minimally invasive surgical techniques and diagnostic tests and is an invaluable tool for both its therapeutic and diagnostic benefit. Therapeutic radiation is used to treat cancers by delivering high doses of ionizing radiation to solid tumors, and diagnostic radiation imaging has been adapted for use in a broad range of medical disciplines including 2D conventional X-ray, 3D Computed Tomography (CT), and real-time

X-ray fluoroscopy imaging. Furthermore, interventional radiology has become its own medical specialty, and in many cases, constitutes an entire department within a modern hospital. Consequently, new materials to be used as X-ray contrast agents (XCAs), X-ray therapeutics, and in radiation shielding garments, have become an intensifying subject of materials research and development.

The X-ray attenuating and shielding properties of a given material are a function of the atomic number, density, and electron configuration of the interacting material. Neglecting K-edge effects, the general equation for the X-ray attenuation coefficient (μ) of an element is described in Eq. (1), where Z is atomic number, A is atomic mass, ρ is density, and E is the incident photon energy [1].

$$\mu = \frac{\rho Z^4}{AE^3} \qquad (1)$$

However, X-ray radiation interacts with materials not only through scattering, but also by the photoelectric effect, which occurs at quantized energies characteristic of the atoms present. Thus, a general relationship between atomic number or density and X-ray attenuation is confounded by K-edge effects, where the K-edge is the energy of electrons in the K-shell with principle quantum number equal to 1. When an incident X-ray is at this energy (e.g., 90 keV for bismuth), it has a high probability of being absorbed, which results in a sharp increase in attenuation of incident photons. Furthermore, diagnostic X-ray imaging is typically performed with an X-ray tube voltage between 10 and 150 kVp, dependent on anatomical characteristics such as specimen thickness, and utilizes an energetically broad range of X-ray photons (**Figure 1A**) [2].

Including both scattering and photoelectric effects, plots of the calculated (i.e., theoretical) mass attenuation as a function of X-ray tube voltage are shown in **Figure 1B** for tungsten, lead and bismuth, where it can be seen that lead and bismuth have fairly similar X-ray attenuation per unit density over the majority of the incident photon range. In contrast, tungsten
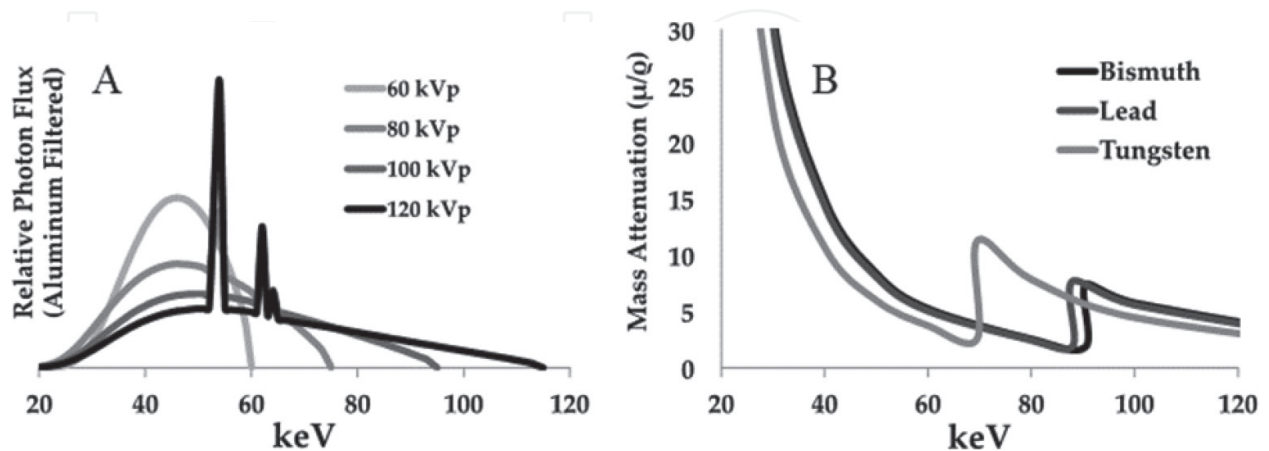
Figure 1. (A) The relative X-ray photon flux produced from a typical medical X-ray tube as a function of the X-ray tube voltage (kVp) after aluminum filtering, which removes lower energy X-rays. (B) The mass attenuation coefficient (μ/ρ) for bismuth, lead, and tungsten is shown as a function of X-ray photon energy (keV).

has a lower mass attenuation than lead or bismuth, except in the range of 70–88 keV, where the K-edge effect increases the attenuation. However, keeping in mind that the incident photon flux of a medical X-ray instrument is polychromatic and dependent on the X-ray tube voltage, predicting quantitative contrast for compositionally different attenuating materials used under different instrumental conditions is difficult. Nonetheless, it is generally true that high Z, dense materials will attenuate X-rays to a greater extent relative to low Z, sparse materials, which makes inorganic nanoparticles attractive as X-ray imaging agents and shielding materials. Nanoparticles of elements such as tungsten ($Z = 74$), gold ($Z = 79$), lead ($Z = 82$) and bismuth ($Z = 83$), as well as compounds of these elements, have been considered attractive for this purpose and are the focus of much materials research in this field.

2. Inorganic nanoparticles as biomedical X-ray contrast and therapeutic agents

2.1. Challenges for developing biomedical X-ray-interacting agents

A multitude of challenges must be considered when designing a targeted X-ray-interacting agent for *in vivo* use. This includes how it will selectively and specifically identify its biological target, the dose required to attain X-ray contrast or therapeutic effect, how it will avoid immune response, and possible toxicity.

In terms of the dose required to achieve X-ray contrast, the goal of a targeted XCA for use in CT imaging is to raise the attenuation of a specific biological tissue type (i.e., a solid tumor) by elevating its average atomic number. CT signal strength is measured in Hounsfield Units (HU), where the signal strength of air is designated as −1000 HU and water as 0 HU; the quantitative contrast of an XCA is evaluated in terms of HU per mM (HU/mM) of the agent or attenuating atom. In a 3D reconstructed CT image, each three-dimensional voxel is assigned an HU value indicating its X-ray attenuation. Adjacent tissues can be differentiated by CT when the HU difference between them is at least three times greater than the background noise intensity [3]. Without artificial contrast, bones are clearly visible, but adjacent soft tissues must have substantially different densities to be distinguished.

Clinically available, small molecule XCAs (**Figure 2**), such as iopromide, iohexol, and iobitridol, use iodine ($Z = 53$) to increase the average atomic number of a tissue, and consequentially its HU value. These agents are limited to systemic imaging, as opposed to targeted imaging, since they are hampered by rapid kidney clearance from the bloodstream and a small number (<10) of high Z atoms per molecule. The quick renal clearance means that a radiologist must image a patient with precise timing relative to contrast agent injection. Additionally, long exposure times are commonly required for CT imaging, necessitating that the agent be delivered continuously during the procedure to ensure adequate contrast; this extended administration can result in kidney damage [4]. Furthermore, solutions of these agents are generally highly viscous at concentrations sufficient to give rise to contrast, resulting from the fact that CT imaging is poorly sensitive to contrast agent detection.
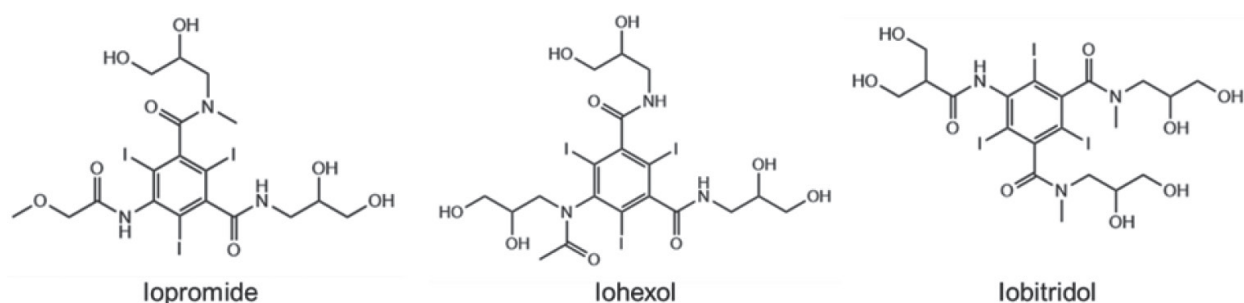
Figure 2. Three examples of iodine-based contrast agents currently in clinical use.

The limitations of current small molecule imaging agents drive the development of new XCAs that can deliver greater per unit contrast to specified biological targets, with longer blood circulation half-lives and less viscous agent doses. Thus, to overcome the high limit of detection of current, small molecule imaging agents and the low sensitivity of CT imaging, nanoparticles carrying thousands or millions of high Z atoms (**Figure 3**) may provide the requisite advantage and enable targeted CT imaging. So far, a variety of inorganic nanoparticles have been evaluated as potential X-ray attenuating agents, as further discussed in Section 2.2.

In terms of biological fate and toxicology, the bio-distribution and pharmacokinetics of inorganic nanoparticles is a complex topic. For the last decade, the enhanced permeation and retention effect (EPR) has been cited as a reason for nanoparticle accumulation in tumor tissues, a theory that is supported by multiple observations using a variety of types of nanoparticles. The EPR effect is explained by the large size of fenestrations in tumor vasculature, which are believed to enable uptake of particles as large as 200 nm in diameter. However, the EPR effect has been disputed, since many of the *in vivo* demonstrations of it have been performed in mice with transfected tumors, which are not necessarily reflective of naturally-occurring
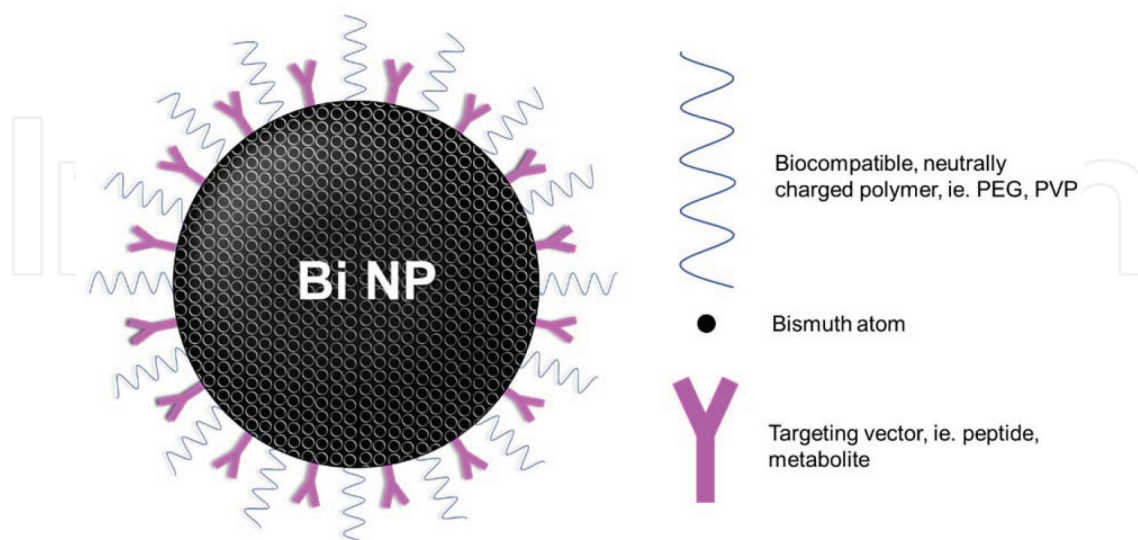
Figure 3. Representation of a targeted Bi NP XCA containing thousands or millions of high-Z bismuth atoms (e.g., a 50 nm Bi NP contains ~1 million Bi atoms). The targeting vector is chosen so that it specifically recognizes a biological receptor, such as a cell surface protein.

human tumors due to their disproportionately large sizes. Further, even in such disproportionately large tumors, low nanoparticle accumulation rates are commonly observed [5, 6].

Despite the absence of well-established principles concerning nanoparticle bio-distribution and fate, several empirically observed trends have been noted and are commonly considered in the design of biomedical agents. When considering the clearance strategy of an intravascularly administered nanoparticle agent, particle size is perhaps the most important variable. It is generally accepted that nanoparticles smaller than 6 nm can be removed by filtration though the kidneys, similar to many small molecules and ions. However, nanoparticles of all sizes can be eliminated by the mononuclear phagocyte system (MPS), a wide-ranging group of cell types that are capable of removing foreign objects from the bloodstream. This occurs due to the accumulation of proteins on the nanoparticle surfaces, which results in identification, uptake, and ultimately clearance by phagocytes. Other factors, including shape, surface charge, and surface chemical functionalities are also important determinants in the identification of nanomaterials by the MPS [7]. To date, a large number of nanoparticles that have been tested in pre-clinical settings have been observed to be sequestered from circulation by the MPS, never reaching their intended target. However, nanoparticles with an electrically neutral surface, and in particular those with polyethylene glycol (PEG) surface coatings, have been shown to accumulate proteins to a lesser extent, which slows MPS recognition and thus enables particles to stay in circulation longer.

2.2. Development of early nanoparticle X-ray contrast agents

The first demonstration of nanoparticles as XCAs was published by Hainfeld et al. [8], where ultra-small gold nanoparticles (Au NPs, ~2 nm) were imaged in an *in vivo* mouse model. The result was the enhancement of X-ray contrast throughout the specimen's entire vasculature 10 min post-injection, followed by eventual renal clearance. Additionally, in mice with transfected tumors, the Au NPs were shown to accumulate preferentially in the tumor, as opposed to healthy tissues, despite the absence of an active targeting molecule on the nanoparticle surfaces. After this study and its follow-up in 2006, Au NPs have been extensively researched as XCAs, as well as for X-ray sensitization (i.e., as agents causing radiation dose enhancement), photo-thermal imaging and therapy, and photo-acoustic imaging [9, 10].

The plethora of biomedical research using Au NPs has been enabled by the development of reliable Au NP synthesis methods, which have resulted in Au NPs with well-defined sizes and low size polydispersity; such Au NP formulations are now readily commercially available. However, while this availability has made Au NPs crucial to the demonstration of nanomaterial-based imaging and therapies, the use of larger Au NPs is limited by poor biological clearance, since elemental gold is quite inert under physiological conditions [11–14]. The oxidative stability of elemental Au presents an apparent advantage in that decomposition products are not expected to interfere with biochemical processes, but also results in the demonstrated disadvantage that Au NPs show high levels of bioaccumulation because they cannot be rapidly degraded into small, molecular species. This has limited several *in vivo* applications, including targeted X-ray imaging, that would benefit from larger (i.e., >6 nm) NPs to achieve detectable radiation interactions.

While many researchers continue to work with Au NPs and look for ways to bypass this issue, there is a widening field of researchers who have focused their work on the development of

bismuth-based nanomaterials as X-ray interactive biomedical agents. A landmark publication demonstrating the use of bismuth-containing XCAs by Rabin et al. illustrated the potential of bismuth(III) sulfide nanoparticles (Bi_2S_3 NPs) in an *in vivo* mouse model [15]. The plate-shaped nanoparticles ranged from 10 to 50 nm on their longest sides, and the surfaces were coated with polyvinylpyrrolidone (PVP), a well-established biocompatible polymer. These PVP-coated Bi_2S_3 NPs showed a superior CT brightness compared to iopromide, a clinically used iodine-based contrast agent, and had a blood circulation half-life of 140 ± 15 min, which is substantially greater than the circulatory half-life of clinical iodinated XCAs. Furthermore, the Bi_2S_3 NP formulation resulted in greater contrast while administered at a lower concentration and as a lower viscosity solution.

Another study of note that utilized Bi_2S_3 NPs as XCAs was performed by Kinsella et al. [16]. In this study, size monodisperse ~10 nm Bi_2S_3 NPs were prepared and surface-coated with the amphiphilic polymer 1,2-distearoyl-*sn*-glycero-3-phosphoethanolamine-N-(amino(polyethylene glycol)) (DSPE-PEG) to produce an uncharged, hydrophilic product. The DSPE-PEG-coated Bi_2S_3 NPs were further conjugated to the LyP-1 peptide, which is a surface antigen for the p32 protein that is over-expressed in several human carcinomas. The accumulation of DSPE-PEG-coated Bi_2S_3 NPs in the tumor was observed to be increased by 70% with the addition of the LyP-1 targeting peptide, although both targeted and untargeted NPs produced adequate contrast to image the tumor. Ultimately, the DSPE-PEG-coated Bi_2S_3 NPs were removed by the hepatic/fecal route, as evidenced by the enhanced contrast of the intestines after a 7-day period. Overall, this publication demonstrated that: (1) even with a fairly small bismuth-based XCA in which the high Z bismuth payload is diluted by sulfur ($Z = 16$), contrast can be superior to that found in commercial iodinated XCAs, and (2) peptide-mediated active tumor targeting can increase efficacy when designing an intravenous agent.

Despite the successful demonstrations of Au and Bi_2S_3 NPs as XCAs, elemental bismuth nanoparticles (Bi NPs) can be argued to have significant advantages that make them potentially more promising as targeted XCAs. Relative to Au and Bi_2S_3, elemental Bi has a higher overall average atomic number, thus taking greater advantage of the general Z^4 increase in X-ray attenuation. Additionally, elemental Bi is semi-stable with respect to oxidative dissolution, making it more readily biodegradable relative to Bi_2S_3 and Au, and therefore potentially permitting the use of larger particles. Furthermore, the degradation of elemental bismuth into bismuth ions (Bi^{3+}) at physiological pH is expected to occur slowly enough to ensure that the concentration of Bi^{3+} in the blood stays below toxic levels, and the resulting Bi^{3+} complexes are expected to be small and highly biocompatible, thus presenting the opportunity for renal clearance [17, 18]. Finally, similar to many nanoparticles composed of other elements, elemental Bi shares the ability to absorb X-ray, visible, and near-IR radiation, which presents opportunities for additional imaging and treatment modalities that use longer wavelength radiation compared to X-rays.

The remainder of this chapter includes summarizing currently published synthetic strategies for producing aqueous Bi NPs and reviews the biomedical research that has so far explored these materials as XCAs, photo-therapeutic agents, and X-ray shielding materials in biomedical settings. Lastly, we discuss the future of Bi NPs in medical imaging and therapeutic technologies.

3. Bi nanoparticles for *in vivo* X-ray applications

3.1. General synthesis considerations for producing medically useful Bi nanoparticles

While Bi NPs are a desirable platform for *in vivo* X-ray contrast and therapeutic applications owing to their dense, un-diluted payload of high Z atoms, synthesis of these materials is generally more difficult and less versatile than other high Z nanomaterials. This is most notable in contrast to precious metal nanoparticles of gold, silver, and platinum, which have high oxidative stability. The primary difficulty in synthesizing elemental Bi NPs is oxidative decomposition, which has led to a prevalence of anaerobic synthetic strategies to prevent oxidation by O_2. These methods often utilize air-sensitive or pyrophoric reagents in the reduction of a Bi^{3+} precursor in the presence of surface-terminating ligands. Furthermore, apolar solvents and hydrophobic ligands are most frequently used to avoid oxidative dissolution of the reduced Bi NPs by H_2O, which results in products that are not water-dispersible as-prepared. Thus, further ligand coating or polymer wrapping is a common strategy to render stable, aqueous Bi NPs, although such strategies result in less X-ray dense particles with additional pharmacological complexity.

We have recently reviewed Bi NP synthesis methods that produce some of the lowest polydispersity hydrophobic and hydrophilic Bi NP colloids at this time, with their associated size metrics (see Supporting information of reference [19]). However, research by our group and several others, has focused on the synthesis of Bi NPs in aqueous or otherwise polar conditions, as well as scalable production. In general, published aqueous and polar phase syntheses of Bi NPs have rarely approached the colloidal stability, chemical stability, and size monodispersity observed in anaerobic, apolar systems. Nonetheless, a few notable synthetic methods have produced aqueous colloids of Bi NPs that are potentially biomedically useful, which are further discussed in Sections 3.2 and 3.3.

3.2. Syntheses of hydrophilic bismuth nanoparticles and demonstration as CT contrast agents

In a polar phase Bi NP synthesis method developed by our group, Bi^{3+} (from Bi(III) nitrate) was reduced by co-reductants morpholine borane and glucose using 1,2-propanediol as solvent to result in hydrophilic Bi NPs in a single step. The resultant Bi NPs (**Figure 4A**) were observed to have an average diameter of 74 ± 14 nm by transmission electron microscopy (TEM), [20] and it was determined that the presence of the reducing sugar (i.e., glucose) in the formulation enhanced Bi NP oxidative stability in the resulting aqueous colloids. This synthetic method has several attractive features for biomedical usage, including a substantial product yield, reproducibility in the size and size distribution of the products obtained, and use of low cost reagents that are relatively biologically benign. Furthermore, because a polymeric surface stabilizer is not used, the Bi core constitutes the majority of the overall particle volume, representing a dense X-ray opaque payload.

We have shown that the oxidative stability of the Bi NPs prepared in this way is sensitive to pH, with the Bi NPs decomposing into soluble Bi^{3+} species at physiological pH (7.4) within
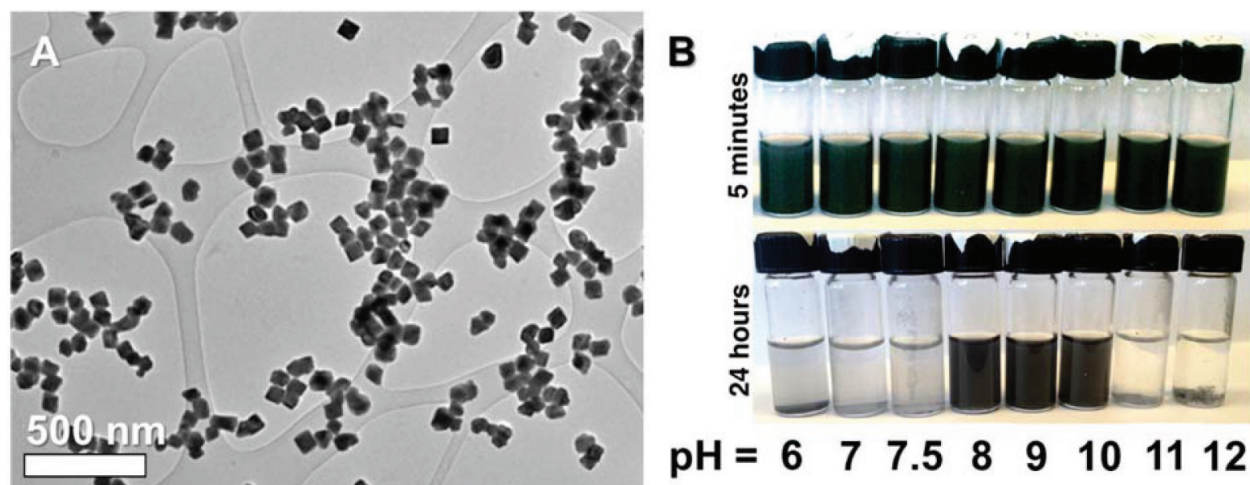
Figure 4. (A) TEM image of Bi NPs synthesized *via* reaction of morpholine borane and glucose with bismuth (III) nitrate in 1,2-propanediol. (B) Photographs showing pH stability of the Bi NPs 5 min (top) and 24 h (bottom) after they are dispersed into aqueous solution (reprinted with permission from reference [21]).

24 h (**Figure 4B**) [21]. This observation suggests a possible mechanism for biological clearance, which has been a substantial clinical translation hurdle for Au NPs. The glucose-stabilized Bi NP colloids were also tested *in vitro*, where no observable cytotoxicity was observed within 1 h in either a cancer or a macrophage cell line at concentrations up to 0.5 mg/mL, suggestive of good biocompatibility. However, at 24 h, the macrophage cell line viability dropped, having an LD50 of 50 μg/mL due to an observed high concentration of internalized Bi NPs.

In a study of quantitative contrast using a clinical CT scanner to image a non-biological phantom (**Figure 5A**), the Bi NPs produced by this method were shown to generate an X-ray contrast of approximately 6 HU/mM Bi (**Figure 5B** and **C**), which is greater at all kVp in comparison to an iodine-based standard, and more than double that of the iodine-based standard at 140 kVp (**Figure 5C**). Additionally, the quantitative X-ray contrast of the Bi NPs was observed to be relatively insensitive to the operating voltage of the CT scanner, performing similarly over the range of 80–140 kVp, while the contrast of an iodinated agent decreased sharply with increasing operating voltage (**Figure 5C**). This synthesis method has since been used and further modified to produce Bi NPs that have been studied *in vivo*. [22, 23]

Li et al. adapted the synthesis method described above to demonstrate X-ray contrast *in vivo* using ~40 nm Bi NPs, which had been additionally PEG-coated to further increase biocompatibility [23]. In non-biological phantom studies, these PEG-coated Bi NPs generated 3.7 times as much contrast as equimolar iopromide, with the measured X-ray attenuation being 60.3 HU/(mg/mL) for the Bi NPs as compared to 16.4 HU/(mg/mL) for the iodinated agent under the same instrumental conditions. *In vitro*, no marked cytotoxicity was observed in either a cancer or an endothelial cell line at concentrations up to 300 μg/mL, although endocytosis was observed, as we also noted. In an *in vivo* study of tumor bearing mice, the PEG-coated Bi NPs were injected intravascularly and were observed to slowly accumulate in tumor tissue over the course of 6 hours, at which time the CT contrast was highest. This degree of non-targeted accumulation in a tumor is higher than that of smaller Bi NPs and was attributed to the EPR effect.
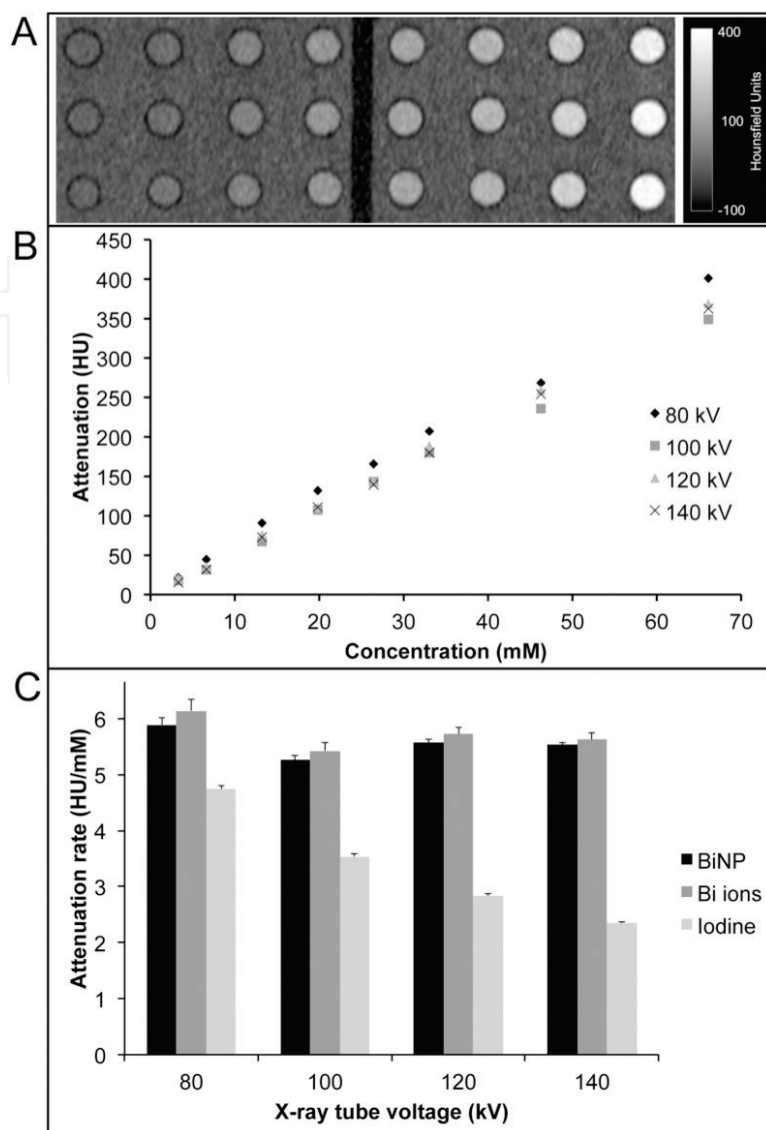
Figure 5. (A) CT image of a concentration gradient of aqueous Bi NP solutions suspended in a non-biological phantom, ranging from 0 to 70 mM Bi in the wells from left to right. (B) The CT attenuation of Bi NP solutions as a function of Bi atom concentration at various operating voltages. (C) Attenuation rates of Bi NPs, ionic bismuth, and ionic iodine in water at various operating voltages. Reprinted from reference [20] with copyright permission from the American Chemical Society. The full text of the article can be found at https://pubs.acs.org/doi/full/10.1021/cm500077z and further permissions related to this material should be directed to the ACS.

However, this observation may in part be due to the large size of the Bi NPs, which are expected to have a long circulation half-life in the bloodstream prior to renal clearance.

Another synthesis method used to make Bi NPs in polar media was developed by Lei et al., which accomplished the reduction of Bi^{3+} using $NaBH_4$ in a glycerol/ethanol solvent mixture and used polyvinylpyrollidone (PVP) to control size [24]. Since the PVP-coated Bi NPs were hydrophilic as-prepared, no further surface modification was required for *in vitro* or *in vivo* work, although the addition of 5 wt% glucose to aqueous solutions of these Bi NPs was also tested. The resultant PVP-coated Bi NPs had an average core diameter of 2.7 ± 1.1 nm by TEM, which is notably substantially smaller compared to the Bi NPs discussed above. However, in non-biological phantoms, dispersions containing the ultra-small, PVP-coated Bi NPs provided approximately 2 times greater contrast than equimolar iobitridol at 120 kVp, with the measured X-ray attenuation

being 7.1 and 3.9 HU/mM for the Bi NP and iobitridol samples, respectively. This study did not observe cytotoxicity in *in vitro* studies using up to 500 μg/mL Bi NP samples.

Lei et al. first assessed the *in vivo* CT contrast of the ultra-small, PVP-coated Bi NPs by intra-tumoral injection, which showed exceptional CT contrast for the tumor. Encouraged by these results, the Bi NPs were administered intravenously and the bio-distribution was monitored. The *in vivo* bio-distribution studies revealed some accumulation in the liver and spleen that had decreased by the 24-h time point, while continued accumulation up to 24 h was observed in the tumor. The HU value of the tumor tissue was observed to increase slowly from 30.3 HU before injection to 53.8 HU at 24 h post-injection, suggesting a slow and passive accumulation of the nanomaterial in the tumor. The Bi NPs were apparently excreted intact within 7 days. Further, using a healthy specimen, a complete blood panel done following an *in vivo* bio-distribution assay revealed that the Bi NP-treated tissues were not significantly different relative to untreated specimens. The further demonstration of a therapeutic application of these ultra-small, PVP-coated Bi NPs is discussed in Section 3.3.

A study by Yu et al. also applied ultra-small Bi NPs as both an XCA and a therapeutic agent [25]. In this study, Bi NPs with an average diameter of 3.6 nm were synthesized by hot injection of a solution containing Bi^{3+} into oleylamine, which acted as solvent, reducing agent, and surfactant. These initially hydrophobic Bi NPs were then made hydrophilic by coating with DSPE-PEG, and further functionalized by covalently attaching LyP-1, a peptide that associates with membrane proteins over-expressed in some cancerous cells. In non-biological phantoms, the Bi NPs generated approximately 3 times greater contrast than equimolar iohexol, with the measured attenuation rates being 13.8 and 4.28 HU/mM for the Bi NPs and iohexol at 80 keV, respectively. Upon intra-tumoral injection, the Bi NP-loaded tumor was clearly visible by CT imaging, having a voxel intensity of >1000 HU, though this result is not extensible to intravenous (IV) administration. However, the bio-distribution and extent of tumor accumulation after IV injection was also examined, which is discussed in Section 3.3 in the context of the use of the LyP-l-DSPE-PEG-coated Bi NPs as a photo-therapeutic agent.

Overall, in the studies noted above, hydrophilic Bi NPs universally outperformed iodinated XCAs by two- to four-fold in terms of contrast at fixed concentrations and had greater blood-circulation half-lives, which demonstrated promise for the use of Bi NPs as lower-dose systemic X-ray contrast agents. Further, the extent of passive tumor accumulation and CT contrast observed in *in vivo* studies demonstrated the possibility of using the Bi NPs to discern diseased tissues, which can be further enhanced by active tumor targeting, i.e., by the addition of pathology-specific recognition groups to the Bi NP surfaces. Additionally, bio-distribution studies of ultra-small (<6 nm) Bi NPs showed that they are cleared largely through the kidneys [24, 25], while larger Bi NPs tend to be cleared hepatically [22, 23]. In addition to their promising application in CT imaging, other biomedical utilities of aqueous Bi NP colloids are further discussed in Section 3.3.

3.3. Applications of Bi nanoparticles in therapeutics

As many nanomaterials have been shown to accumulate in solid tumors, the use of photon therapies that can excite a functional nanomaterial to produce a local and lethal effect on surrounding cells is an active area of cancer research.

One example of a photon therapy is photo-thermal therapy, which uses near infrared (NIR) or visible radiation to raise the local temperature of a biological tissue above 48°C, leading to irreversible protein denaturation and aggregation within 4–6 min [26]. NIR radiation is of particular utility in the field of photon therapeutics due to relatively long wavelengths that result in large (~10 mm) tissue penetration depths and low tissue ionization. Bi NPs broadly absorb both visible and NIR radiation, and afterwards vibronically relax to produce heat, which makes Bi NPs a candidate for use as NIR-photo-thermal therapy enhancement agents.

The above referenced study by Lei et al. demonstrated the use of Bi NPs for photo-thermal imaging and therapy [24]. As aqueous colloids, the NIR-to-thermal conversion efficiency of ~3 nm PVP-coated Bi NPs was determined to be as high as 30%, which is higher than for other photo-thermal agents including gold nanoparticles. In a preliminary *in vivo* study using tumor-bearing mice (having both experimental and control specimens), the efficacy of Bi NPs as photo-thermal agents was established by IV administration of 20 mg/kg Bi NPs, which passively accumulated in the tumor of the experimental specimen over the course of 24 h. After 24 h, both control and experimental specimens were subjected to NIR photo-therapy using 808 nm incident light at a power of 1.3 W/cm^2; the temperature of the tumors was monitored using an IR camera. Within 6 minutes, a temperature change of 25°C (to ~65°C) was observed in the tumor tissue of the Bi NP-treated specimen, while the temperature of the control specimen had only increased modestly (<5°C). In further *in vivo* experiments, infrared cameras were used to image the tumor temperature of specimens in four groups, as follows: (1) those not treated with Bi NPs or NIR light, (2) those treated with NIR light only, (3) those treated with Bi NPs (by IV injection) only, and (4) those treated with both NIR light and Bi NPs (by IV injection). The photo-thermal treatment, when applied, delivered 808 nm incident light at a power of 1.3 W/cm^2 and was administered 24 h following the Bi NP injections. For specimens in these groups, the relative tumor volume was monitored over a period of 14 days, and it was observed that in the groups treated with only Bi NPs or only NIR light, the tumor volumes grew at the same rate as the untreated control. However, a significant growth inhibition (~10% the size of the other groups) was observed for the group receiving Bi NPs in combination with NIR therapy, which demonstrated that the local heating correlated with cancer tissue death. Overall, these results showed that ultra-small, passively accumulating Bi NPs could be useful as a photo-thermal therapy agent.

Another possible therapeutic application for Bi NPs is their use in radiation dose enhancement during X- or gamma-ray treatments. Currently in the United States, over half of all cancer patients will receive a form of radiation therapy, typically using extremely high-energy photons in the MeV range. The drawback of this type of treatment is damage incurred to surrounding healthy tissues, which typically limits the radiation doses delivered to patients. Thus, there is a desire to lower the radiation dose delivered to patients while maintaining the efficacy of the radiation therapy for the treatment of cancers. To address this limitation, the development of materials that can enhance the local ionizing effects of radiation could make these treatments substantially more effective. So far, several nanomaterials (e.g., gold nanoparticles and hafnium oxide nanoparticles) have demonstrated an increase in local ionizing damage when used with keV radiation in small animal models, and some are currently in clinical trials [27–32]. However, as outlined above in the context of XCAs, bismuth has

a number of unique advantages for biomedical applications, which should remain true for their application as radiation dose enhancing nanoparticles. Furthermore, not only do Bi NPs attenuate X-rays far more efficiently than soft tissue, they have also been shown to produce photo-generated, ionizing chemical species, which can potentially be leveraged to contribute cellular damage. The mechanisms by which nanoparticles enhance cellular damage from radiation likely involves a multitude of reactions, and is a topic of current investigation [27].

Two groups have recently demonstrated the ability of Bi NPs to multiply local radiation ionization events upon excitation by X-rays in the keV energy range. For example, Yu et al. co-administered 3.6 nm DSPE-PEG-coated Bi NPs with a single dose of 4 Gray (Gy) radiation to tumor-bearing mice. [25] After 14 days, tumor growth rates of the Bi NP/radiation-treated mice-were 33% lower than those treated by radiation alone. In the same study, Yu et al. also found that Bi NPs collected from the urine and feces of mice 24 h after injection had the same size and morphology as when they were initially injected, demonstrating that the 3.6 nm DSPE-PEG-coated Bi NPs can be cleared but not significantly degraded in this timeframe [25]. Another study by Deng et al. showed similar results using 50 nm PVP-coated, untargeted Bi NPs, slowing tumor growth by 43% over a 14 day period. [22] Further modification was performed on these Bi NPs, including conjugation of the biological-targeting group folate and encapsulation within red blood cell membranes. Here, it should be noted that nanoparticles with folate surface ligands have previously shown increased accumulation in multiple cancerous tissues types that overexpress folate receptors. The authors observed that when the RBC-modified, folate-targeted Bi NPs were used, tumor growth rates were reduced by more than 50% compared to radiation alone, and mouse survival rates over 36 days increased from 0 to 60%.

Overall, the studies of Bi NPs as photo-therapuetic agents have shown that a synergistic combination of NIR or X-ray radiation with intravascularly administered Bi NPs can significantly impact tumor growth rates. In addition, several of these recent *in vivo* studies have included monitoring for possible tissue damage or changes in blood serum concentrations after administration of Bi NPs and radiation [22–25]. These studies have revealed that while tumor tissue samples tend to show damage from the co-administration of Bi NPs and radiation, tissues in the heart, lungs, spleen, liver, and kidneys have all been found to remain undamaged. Thus, the use of Bi NPs in NIR and X-ray photo-therapies may prove useful for increasing the efficacy of these procedures in cancer treatments. Finally, while we have discussed the use of Bi NPs as both imaging and therapeutic agents in the former sections, we end this chapter by discussing the use of Bi nano- and microparticles in macroscopic radiation-attenuating tools, such as personal protective equipment and imaging guides.

4. Bi nano- and microparticles for X-ray shielding in medical applications

4.1. Current status of X-ray shielding materials

There is a substantial call from the medical community for improved radiation shielding garments for medical personnel who regularly work in proximity to high-energy radiation [33].

Increased awareness of the harmful stochastic effects of radiation exposure, coupled with an increase in the number of medical procedures (primarily X-ray fluoroscopy) and the increased X-ray voltages required for imaging larger patients, have raised concerns about accumulated radiation exposure to medical personnel [34, 35]. Research has shown that medical personnel who regularly work with high-energy radiation are particularly susceptible to, and have increased incidences of, specific types of cancer [36]. Because of the ubiquitous use of ionizing radiation in medicine, specialty garments, tools, and devices have been developed, both for protection against the harmful effects of radiation, as well as for use with radiation imaging.

In radiation imaging, such tools include catheters that contain platinum wires for use with fluoroscopic imaging and gold fiducial markers that are surgically embedded in a patient to provide guides in CT imaging and therapeutic radiation delivery [37]. In personal protective equipment, radiation-interacting (or shielding) materials include specialized rooms with lead-lined walls, leaded glass viewing areas, and lead-based radiation protective garments. More recently, specialized drapes and blankets have become available.

Personal radiation shielding garments have historically been composed of lead salts (e.g., $Pb(II)SO_4$) embedded into a plastic matrix to form a wearable composite material. This design results in a hard, brittle composite containing a large percentage of lead salt (>60%) by weight. This composite is then encased between heavy vinyl sheets to keep the lead from contacting the wearer. The weight burden from lead is roughly 50% of the overall garment weight, with the plastic casing composing the remainder. Recently the isolation of lead dust by this design has caused lead aprons to become a suspected source of lead poisoning in medical settings [38]. Lead aprons are the most commonly encountered garment of this type and by design these are worn as an X-ray shield to protect the torso and upper legs, leaving the head, neck, and arms exposed to radiation. Garments designed to shield additional areas, such as thyroid, gonads and breasts, and less commonly, the head and hands, are also sparingly used in medical environments, but are extremely bulky and cumbersome.

Lead is heavy, toxic, and environmentally damaging, which makes it a good candidate for replacement by alternative elements that can provide good X-ray shielding. Lightweight shielding materials containing lower atomic number elements have been developed and are marketed specifically to address the weight burden issue that lead-based garments suffer from. In these products, the lead salt is replaced with a mixture of salts of lighter elements, including barium, tin, tungsten, and some lanthanoids. These garments are tested and marketed as having a "lead shielding equivalent" at a specific tested X-ray voltage. However, when tested over a range of X-ray voltages (kVp), other than the voltage they were optimized for, they can show an inadequate radiation attenuation. [39] X-ray attenuation is reported in "mm of lead" and as a kVp is not specified for this testing, this has enabled manufacturers to report misleading shielding data and has raised concern for medical personnel who rely on these garments for protection [40].

For high performance X-ray contrast devices, such as catheters or other medical devices that are surgically inserted, tungsten particles or platinum wires are generally utilized. Use of these elements also has drawbacks, including difficulty in manufacturing and processing. Tungsten is extremely hard, requiring specialized equipment to process, while platinum is extremely expensive (>$13,000/lb) and is thus limited to use in small devices, such as catheter tips.

Bismuth is an excellent candidate for lead replacement in garments and platinum and tungsten replacement in surgical devices. Relative to lead, it has a similar or higher X-ray attenuation cross-section, but is non-toxic. Bismuth has a lower melting point relative to tungsten (272 vs. 3422°C) and is much softer (2.2 vs. 7.5 Mohs hardness), making it much easier to machine. The challenge with adapting bismuth for use in shielding garments has historically been the price of raw material. Though much cheaper than platinum and somewhat less expensive than tungsten (approximately $20 per pound), bismuth prices have fluctuated widely over the past decades from $3 to $30 per pound, while lead has historically been roughly $1 per pound. Incorporating bismuth particles into medical devices has been explored by device manufacturers, but the low oxidative stability of bismuth during processing has limited manufacture adaptation. However, we have recently developed a method for the production of surface-stabilized Bi nano- and microparticles that are easily polymer-dispersed for use in medical devices and protective garments, which are described in Section 4.2 [41].

4.2. Fabrication of Bi nano- and micro-composites for X-ray shielding applications

We have recently developed a method to produce microscopic, surface-passivated bismuth particles for the creation of plastic X-ray opaque composites [41]. To produce the surface-passivated, micron-sized bismuth material we utilize high-energy ball milling of bismuth ingot in various organic solvents or other surface coordinating ligands. The organic passivants coat the freshly fractured Bi crystallites, thus minimizing surface oxide formation. Particles produced are of a broad range in size (from a few hundred micrometers, down to the nanometer scale) and can be size selected for a specific application. Excess particles are easily melted on the bench top and the bismuth can be recovered and recycled though the milling and passivating process. Furthermore, the wide choice of organic solvent also permits tuning the particle hydrophilicity and chemical functionality to permit dispersal of the micrometer scale bismuth domains into a variety of plastics. As examples, we have produced hydrophilic bismuth microparticles by milling in the presence of dihydroxyacetone (DHA) and 1,2-propane diol, and hydrophobic bismuth microparticles by milling in the presence of in 1-pentene, or styrene, and toluene. The resulting bismuth microparticles suspended in their milling solvents are generally collected by centrifugation, washed with an appropriate solvent, dried, ground to a fine powder and sieved to collect particles in a narrow size range. Such organic-passivated, size-selected particles can then be mixed into molten or uncured polymers such as silicone, polyurethane, polystyrene, and latex to form X-ray opaque polymer composites **Figure 6**(**A**-**C**). The weight percent of the micron-sized radiopaque filler in these composites can be readily calculated and varied over a wide range. We observed that the bismuth microparticles embedded in these composites do not undergo substantive oxidative decomposition, nor do they aggregate within the polymeric matrix.

We tested one possible application of such composite materials for the fabrication of radiopaque surgical sponge markers, which are commonly used in surgery to avoid retention of foreign objects [21]. In doing so, we prepared polyurethane composites containing 20, 40, 60, and 85 wt% of our bismuth micron material and compared them to a commercial sponge marker. The commercial sponge marker was produced by Medline Industries and is reported to be a polymer-salt composite of polyvinylchloride containing between 60 and 83% $Ba(II)SO_4$ as the radiopaque filler. Our composites were prepared by mixing uncured liquid polyurethane with
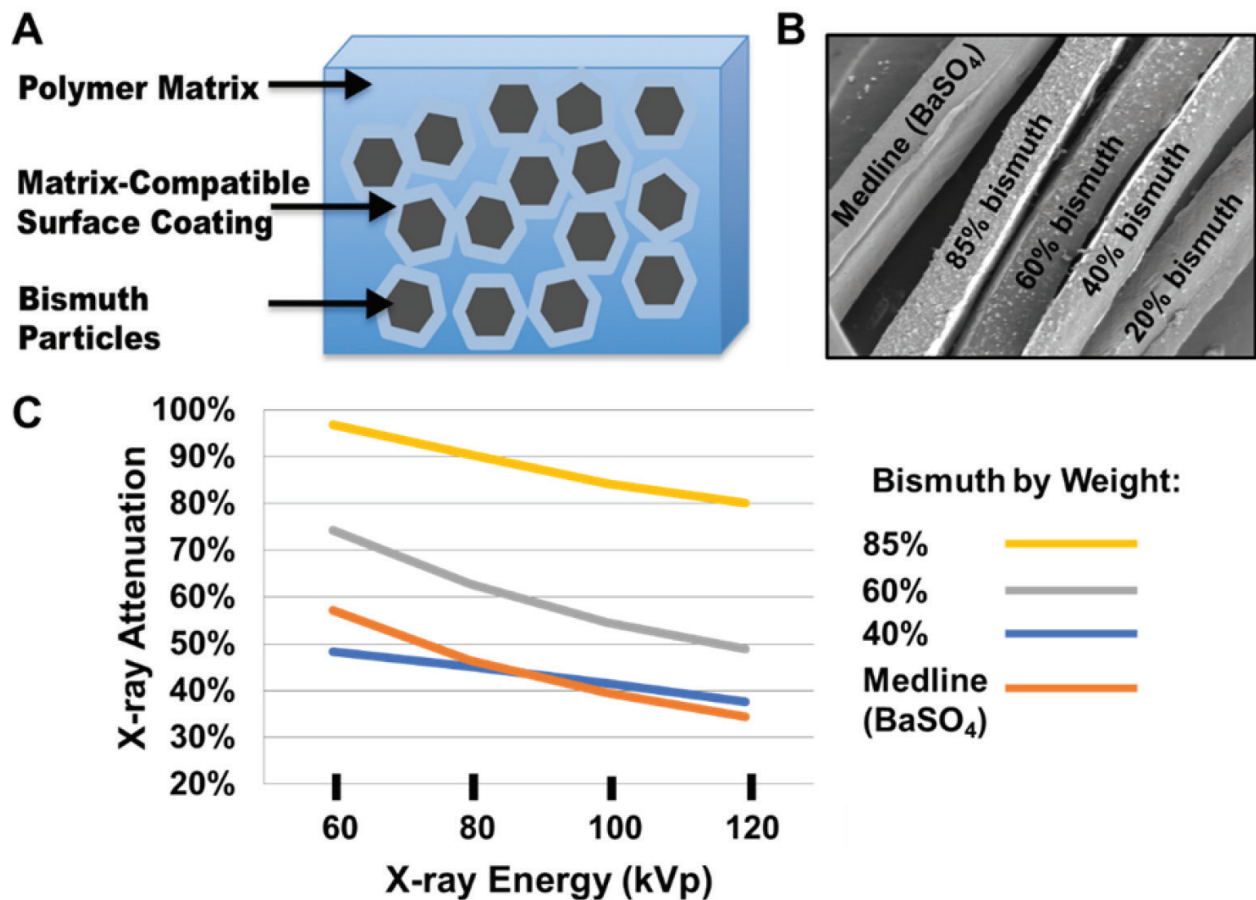
Figure 6. (A) Components of a composite X-ray shielding material. (B) SEM of polymer/filler composite materials with varied mass percent of filler (bismuth microparticles or BaSO$_4$). (C) X-ray attenuation of bismuth microparticle- and BaSO$_4$-containing X-ray shielding materials at various operating voltages (reprinted with permission from reference [21]).

dried, sieved DHA-coated bismuth microparticles, and the resulting mixture was molded using Teflon plates to produce a "ribbon" of similar thickness to the commercial sponge marker.

To compare attenuation of the commercially available surgical sponge marker to the bismuth composite markers, X-ray attenuation measurements were performed by an external analytical laboratory across a range of medically relevant incident photon energies. The composite samples tested were 0.56, 0.55, 0.51 and 0.64 mm thick for the Medline, 40, 60 and 85% by weight bismuth markers, respectively. The attenuation of the commercial composite only exceeded the attenuation of the 20% bismuth composite across all energies, and the 40% bismuth composite at incident photon energies below 80 kVp. However, superior attenuation across all voltages was observed for the 60 and 85% bismuth composites as compared to the commercial composite. For the 85% bismuth composite, the percent X-ray attenuation was nearly 100% at 60 kVp, more than double that of the commercial marker. Further, the 85% bismuth marker was determined to have a lead equivalent X-ray attenuation of 0.21 mm, which would indicate that a 1.2 mm thick sheet of the 85% bismuth composite material would provide similar radiation protection to the lead aprons commonly used in medical facilities (0.5 mm lead equivalent attenuation) [38]. While this is thicker than a sheet of solid lead, the low toxicity of bismuth means that the

shielding material can be placed directly against the skin, and will not require thick protective layers around the functional material. As a substantial portion of the weight burden from lead shielding garments is a result of the vinyl sheeting required to isolate the lead, we estimate that a bismuth particulate shielding garment would be roughly half the weight of a lead garment.

We expect the radiopaque bismuth micromaterial filler we have produced will find use in a variety of thin, flexible plastic composites that can be molded into 3D shapes (such as hats, gloves, or long-sleeved shirts) to provide an improved form factor relative to current technologies. Fabrication of thin, flexible X-ray opaque composite materials should enable better engineering of shielding garments, specifically in regards to the weight burden and flexibility restriction on the wearer.

5. Summary and prospectus for the future of bismuth nano- and microparticles in biomedical X-ray applications

New synthetic methods for producing hydrophilic Bi NPs in the 2–100 nm size range are increasingly reported. As interest in adapting new nanomaterials for biomedical applications continues to grow, it is expected these materials will be further explored and find new niche applications or facilitate development of new technologies in nanomedicine. Bismuth nanoparticles have demonstrated superior X-ray contrast by CT imaging, which exceeds the clinical standard of iodinated X-ray contrast media by 2–4-fold. This may permit the use of systemically administered Bi NPs as lower dose, lower viscosity, and lower toxicity contrast agents. The passive accumulation of untargeted Bi NPs in tumors has demonstrated a high tumor CT signal and has been shown to provide a means of sensitizing cancer tissues to local radiation damage using NIR and X-ray photo-therapies. Additionally, the replacement of lead in personal shielding garments has the potential for development of new and more practical personal protective equipment. The high biocompatibility, low cost, and exceptional X-ray attenuation of bismuth make this unique element a rising star in the application of new technologies in radiation medicine.

The future of hydrophilic Bi NP contrast and therapeutic agents will likely see more active biological targeting studies, with the goal of using Bi NPs to selectively and specifically seek out known biochemical markers of disease. The specific biomarkers of disease that are the target of molecular imaging and therapy are known to be present at low concentrations (10^{-9} to 10^{-10} M), necessitating that the imaging modality used is capable of detecting imaging agents at similarly low concentrations [42]. Since the limit of detection of CT imaging is high, this would necessitate the delivery of a large number of X-ray attenuating atoms to a highly localized area, which may be possible with pathology-targeted, high Z nanoparticles. To estimate how many Bi NPs this would require, achieving a 100 mM concentration of Bi in a 1 mm^3 volume would require 10^{-7} mol of Bi, which for uniform 150 nm Bi NPs is approximately 10^9 Bi NPs. Given a reasonable tumor cell density of 10^6–10^7 cells/mm^3, 1–10 Bi NPs per tumor cell would be needed [43]. Further bio-distribution studies of IV injected pathology-targeted Bi NPs would be needed to determine whether this is possible, and to establish the actual limit of detection.

In the majority of the studies reviewed above, favorable *in vitro* and *in vivo* biocompatibility was observed for hydrophilic Bi NPs. However, so far, only ultra-small Bi NPs have a predictable and practical biological clearance mechanism *via* renal filtration, while the larger Bi NPs that could be most useful as targeted imaging agents are unpredictably endocytosed. Endocytosis of larger Bi NPs may be useful if they are selectively uptaken by disease tissue and used in a photo-dynamic therapies, but this would be limiting in a targeted imaging application. Consequently, further research may involve the encapsulation of ultra-small Bi NPs into larger structures, such as blood cells, liposomes, polymeric aggregates and other nano-sized drug-delivery motifs. The goal would be to maximize the overall aggregate signal in a small volume host, while permitting renal clearance of the payload after release from the host. Alternatively, the use of large Bi NPs may be achievable if surface stabilization strategies or appropriate formulations could be designed to control the rate of oxidative dissolution of the Bi NPs.

Acknowledgements

Conflict of interest

The authors declare no competing financial or other conflicts of interest.

Author details

Hayden Winter, Anna L. Brown and Andrea M. Goforth*

*Address all correspondence to: agoforth@pdx.edu

Department of Chemistry, Portland State University, Portland, OR, USA

References

[1] Lusic H, Grinstaff MW. X-ray-computed tomography contrast agents. Chemical Reviews. 2013;**113**(3):1641-1666

[2] US Department of Commerce, N. NIST: X-Ray Mass Attenuation Coefficients. http://www.nist.gov/pml/data/xraycoef/index.cfm

[3]   Mukundan S, Ghaghada KB, Badea CT, Kao C-Y, Hedlund LW, Provenzale JM, et al. A liposomal nanoscale contrast agent for preclinical CT in mice. American Journal of Roentgenology. 2006;**186**(2):300-307

[4]   McCullough PA. Contrast-induced acute kidney injury. Journal of the American College of Cardiology. 2008;**51**(15):1419-1428

[5]   Wilhelm S, Tavares AJ, Dai Q, Ohta S, Audet J, Dvorak HF, et al. Analysis of nanoparticle delivery to tumours. Nature Reviews Materials. 2016;**1**(5):16014

[6]   Nakamura Y, Mochida A, Choyke PL, Kobayashi H. Nanodrug delivery: Is the enhanced permeability and retention effect sufficient for curing cancer? Bioconjugate Chemistry. 2016;**27**(10):2225-2238

[7]   Gustafson HH, Holt-Casper D, Grainger DW, Ghandehari H. Nanoparticle uptake: The phagocyte problem. Nano Today. 2015;**10**(4):487-510

[8]   Hainfeld JF, Slatkin DN, Smilowitz HM. The use of gold nanoparticles to enhance radiotherapy in mice. Physics in Medicine and Biology. 2004;**49**(18):N309-N315

[9]   Hainfeld JF, Slatkin DN, Focella TM, Smilowitz HM. Gold nanoparticles: A new X-ray contrast agent. The British Journal of Radiology. 2006;**79**(939):248-253

[10]   Yang X, Yang M, Pang B, Vara M, Xia Y. Gold nanomaterials at work in biomedicine. Chemical Reviews. 2015;**115**(19):10410-10488

[11]   Kennedy LC, Bickford LR, Lewinski NA, Coughlin AJ, Hu Y, Day ES, et al. A new era for cancer treatment: Gold-nanoparticle-mediated thermal therapies. Small. 2011;**7**(2): 169-183

[12]   Khlebtsov N, Dykman L. Biodistribution and toxicity of engineered gold nanoparticles: A review of in vitro and in vivo studies. Chemical Society Reviews. 2011;**40**(3):1647-1671

[13]   Alkilany AM, Murphy CJ. Toxicity and cellular uptake of gold nanoparticles: What we have learned so far? Journal of Nanoparticle Research. 2010;**12**(7):2313-2333

[14]   Kamat PV. Photophysical, photochemical and photocatalytic aspects of metal nanoparticles. The Journal of Physical Chemistry. B. 2002;**106**(32):7729-7744

[15]   Rabin O, Manuel Perez J, Grimm J, Wojtkiewicz G, Weissleder R. An X-ray computed tomography imaging agent based on long-circulating bismuth sulphide nanoparticles. Nature Materials. 2006 Feb;**5**(2):118-122

[16]   Kinsella JM, Jimenez RE, Karmali PP, Rush AM, Kotamraju VR, Gianneschi NC, et al. X-ray computed tomography imaging of breast cancer by using targeted peptide-labeled bismuth sulfide nanoparticles. Angewandte Chemie International Edition. 2011;**50**(51):12308-12311

[17]   Longmire M, Choyke PL, Kobayashi H. Clearance properties of nano-sized particles and molecules as imaging agents: Consideration and caveats. Nanomedicine (London, England). 2008;**3**(5):703-717

[18] Alexis F, Pridgen E, Molnar LK, Farokhzad OC. Factors affecting the clearance and bio-distribution of polymeric nanoparticles. Molecular Pharmaceutics. 2008;**5**(4):505-515

[19] Winter H, Christopher-Allison E, Brown A, Goforth A. Aerobic method for the synthesis of nearly size- monodisperse bismuth nanoparticles from a redox non-innocent precursor. Nanotechnology. 2018;**29**(15):155603

[20] Brown AL, Naha PC, Benavides-Montes V, Litt HI, Goforth AM, Cormode DP. Synthesis, X-ray opacity, and biological compatibility of ultra-high payload elemental bismuth nanoparticle X-ray contrast agents. Chemistry of Materials. 2014;**26**(7):2266-2274

[21] Brown A. Bismuth Nanoparticles as Medical X-Ray Contrast Agents: Synthesis, Characterization and Applications. Portland, OR: Portland State University; 2013

[22] Deng J, Xu S, Hu W, Xun X, Zheng L, Su M. Tumor targeted, stealthy and degradable bismuth nanoparticles for enhanced X-ray radiation therapy of breast cancer. Biomaterials. 2018;**154**:24-33

[23] Li Z, Liu J, Hu Y, Li Z, Fan X, Sun Y, et al. Biocompatible PEGylated bismuth nanocrystals: "All-in-one" theranostic agent with triple-modal imaging and efficient in vivo photothermal ablation of tumors. Biomaterials. 2017;**141**:284-295

[24] Lei P, An R, Zhang P, Yao S, Song S, Dong L, et al. Ultrafast synthesis of ultrasmall poly(vinylpyrrolidone)-protected bismuth nanodots as a multifunctional theranostic agent for in vivo dual-modal CT/photothermal-imaging-guided photothermal therapy. Advanced Functional Materials. 2017;**1702018**(35):1702018

[25] Yu X, Li A, Zhao C, Yang K, Chen X, Li W. Ultrasmall semimetal nanoparticles of bismuth for dual-modal computed tomography/photoacoustic imaging and synergistic thermoradiotherapy. ACS Nano. 2017;**11**(4):3990-4001

[26] Jaque D, Martínez Maestro L, del Rosal B, Haro-Gonzalez P, Benayas A, Plaza JL, et al. Nanoparticles for photothermal therapies. Nanoscale. 2014;**6**(16):9494-9530

[27] Her S, Jaffray DA. Gold nanoparticles for applications in cancer radiotherapy: Mechanisms and recent advancements. Advanced Drug Delivery Reviews. 2017;**109**:84-101

[28] Retif P, Pinel S, Toussaint M, Frochot C, Chouikrat R, Bastogne T, et al. Nanoparticles for radiation therapy enhancement: The key parameters. Theranostics. 2015;**5**(9):1030-1044

[29] Schuemann J, Berbeco R, Chithrani DB, Cho SH, Kumar R, McMahon SJ, et al. Roadmap to clinical use of gold nanoparticles for radiation sensitization. International Journal of Radiation Oncology, Biology, Physics. 2016;**94**(1):189-205

[30] Nanoparticles comprising metallic and hafnium oxide materials, preparation and uses thereof. NANOBIOTIX; US20140335015A1, 2012

[31] Inorganic nanoparticles compositions in combination with ionizing radiations for treating cancer. US20150374818A1, 2014

[32] Simon V, Ceccaldi A, Lévy L. Activatable nanoparticles for cancer treatment. Nanobiotix. In: Nanoscience. Berlin, Heidelberg: Springer Berlin Heidelberg; 2009. pp. 1121-1141

[33] Schueler BA. Operator shielding: How and why. Techniques in Vascular and Interventional Radiology. 2010;**13**(3):167-171

[34] Klein LW, Miller DL, Balter S, Laskey W, Haines D, Norbash A, et al. Occupational health hazards in the interventional laboratory: Time for a safer environment. Journal of Radiology Nursing. 2010;**29**(3):75-82

[35] Miller DL, Vañó E, Bartal G, Balter S, Dixon R, Padovani R, et al. Occupational radiation protection in interventional radiology: A joint guideline of the cardiovascular and interventional radiology society of Europe and the society of interventional radiology. Journal of Vascular and Interventional Radiology. 2010;**21**(5):607-615

[36] Hricak H, Brenner DJ, Adelstein SJ, Frush DP, Hall EJ, Howell RW, et al. Managing radiation use in medical imaging: A multifaceted challenge. Radiology. 2011;**258**(3):889-905

[37] National Cancer Institute. NCI Dictionary of Cancer Terms. Vol. 1, National Cancer Institute; 2013. p. 1. https://www.cancer.gov/publications/dictionaries

[38] Burns KM, Shoag JM, Kahlon SS, Parsons PJ, Bijur PE, Taragin BH, et al. Lead aprons are a lead exposure hazard. Journal of the American College of Radiology. 2017;**14**(5):641-647

[39] Peters SMB, Zweers D, de Lange F, Mourik JEM. Lead composite vs. nonlead protective garments: Which are better? A multivendor comparison. Radiation Protection Dosimetry. 2017;**175**(4):460-465

[40] Durán A, Hian SK, Miller DL, Le Heron J, Padovani R, Vano E. Recommendations for occupational radiation protection in interventional cardiology. Catheterization and Cardiovascular Interventions. 2013 Jul;**82**(1):29-42

[41] Goforth A, Brown A. Bismuth Particle X-Ray Contrast Agents. U.S. Patent Application No. 14/124236. 2014

[42] De León-Rodríguez LM, Martins AF, Pinho MC, Rofsky NM, Sherry AD. Basic MR relaxation mechanisms and contrast agent design. Journal of Magnetic Resonance Imaging. 2015;**42**(3):545-565

[43] Swy ER, Schwartz-Duval AS, Shuboni DD, Latourette MT, Mallet CL, Parys M, et al. Dual-modality, fluorescent, PLGA encapsulated bismuth nanoparticles for molecular and cellular fluorescence imaging and computed tomography. Nanoscale. 2014;**6**(21): 13104-13112